Inorganic Chemistry

pubs.acs.org/IC
Article

Haptotropic Phenomena in Digold(I) Triple-Bonded Complexes

Ignacio Nieto-Vargas, Juan Cayuela-Castillo, Francisco J. Fernández-de-Córdova, Israel Fernández,* and Pablo Ríos*

Cite This: *Inorg. Chem.* 2026, 65, 7153−7160
Read Online

ABSTRACT: Addition of either IPrAuOTf or IPrCuOTf (IPr = 1,3-bis(2,6-diisopropylphenyl)imidazol-2-ylidene; OTf = trifluoromethanesulfonate anion) to the digold acetylide IPrAuC≡CAuIPr results in the selective formation of the corresponding trimetallic cationic species [IPrAuC≡C(π-MIPr)AuIPr][OTf] (M = Au or Cu). Variable-temperature ^{1}H NMR experiments (VT-NMR) reveal that while the homotrimetallic gold complex exhibits dynamic σ,π-exchange in solution at temperatures even as low as −130 °C, the heterometallic analogue presents a static scenario. On the other hand, extension of the acetylide bridge by one additional acetylide unit using IPrAuC≡C−C≡CAuIPr introduces a new fluxional process in the corresponding analogous trimetallic compounds [IPrAuC≡C(π-MIPr)−C≡CAuIPr][OTf] (M = Au or Cu), namely π,π-exchange. In the case of the copper-containing complex, this exchange occurs even at low temperatures, whereas exchange can be thermally arrested in the trigold system at temperatures below −10 °C. Computational studies indicate that the divergent behavior between gold and copper regarding π,π-exchange does not appear to stem from their interaction with the alkyne fragment but rather in how this interaction changes along the reaction coordinate toward the transition state geometry.

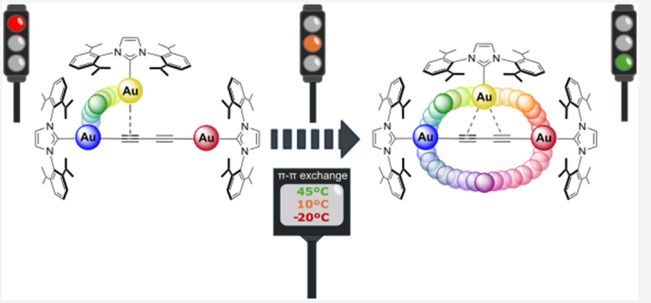

INTRODUCTION

Historically, the field of homogeneous gold(I) catalysis has been primarily centered on the activation of C−C multiple bonds, typically including a single metal center in the catalytic cycle.[1] However, a paradigm shift took place in 2008 when Houk, Toste, and co-workers evidenced that cationic digold(I) σ,π-acetylide complexes are key reactive intermediates in the catalytic cycloisomerization of 1,5-allenynes.[2] This initial discovery spurred the investigation of cationic diaurated species and their role in the catalytic activation of π systems by others. Consequently, this collective effort has dramatically expanded the scope of synthetic strategies that leverage gold in organic chemistry.[3] Nevertheless, there is still ongoing debate regarding the role of cationic digold(I) compounds stemming from the unpredictable reactivity of these species. While some groups have reported examples wherein digold(I) σ,π-acetylide complexes are productive intermediates in catalytic transformations,[2,4] others have demonstrated that digold(I) σ,π-acetylide and/or *gem*-diaurated complexes are off-cycle, dead-ends in catalysis.[4g,5] This unpredictability makes catalyst selection non-obvious and thus hampers rational reaction design.

Moreover, despite the numerous examples of organogold complexes, information on their fluxional phenomena remains limited, which is striking, given that many gold-catalyzed reactions involve thermodynamic equilibria. In the particular case of cationic digold(I) σ,π-acetylides, some examples include equilibria between mono- and diaurated species,[5b] between alkenes and alkynes,[6] competition between π or σ,π activation modes,[7] or equilibria involving coordination of the LAu$^+$ moiety to different alkyne fragments within the same molecule (Scheme 1A).[4,8] Results from the computational investigations of the latter example suggest that the formation of dibenzopentalenes through intramolecular cyclization is possible because an NHC−Au$^+$ (NHC =*N*-heterocyclic carbene) group is able to migrate from a thermodynamically stable σ,π geometry wherein both gold atoms are on the same π system (Isomer **I**, Scheme 1A) to a higher energy isomer **II**, which enables the subsequent steps.[8] Although intermediates like **II** have been previously proposed,[4] this case clearly illustrates how the mobility of the NHC−Au$^+$ is key in the catalytic process, as observed for a similar rearrangement where the computationally proposed mobility of gold across an aryne intermediate determines the observed product (Scheme 1B).[4c] In addition to the positionally fluxional bonding of each NHC-Au$^+$ fragment between different alkyne moieties, the coordination mode between these fragments can also display dynamic behavior, as the triple bond can undergo "slippage" between η^2 and η^1 geometries, with the latter mode exhibiting

Received: October 2, 2025
Revised: November 13, 2025
Accepted: December 1, 2025
Published: December 5, 2025

Scheme 1. (A−C) Representative Examples of Computationally Investigated Fluxional Processes Involving Cationic Au(I) Alkyne Species and (D) Dynamic Phenomena Explored in this Work

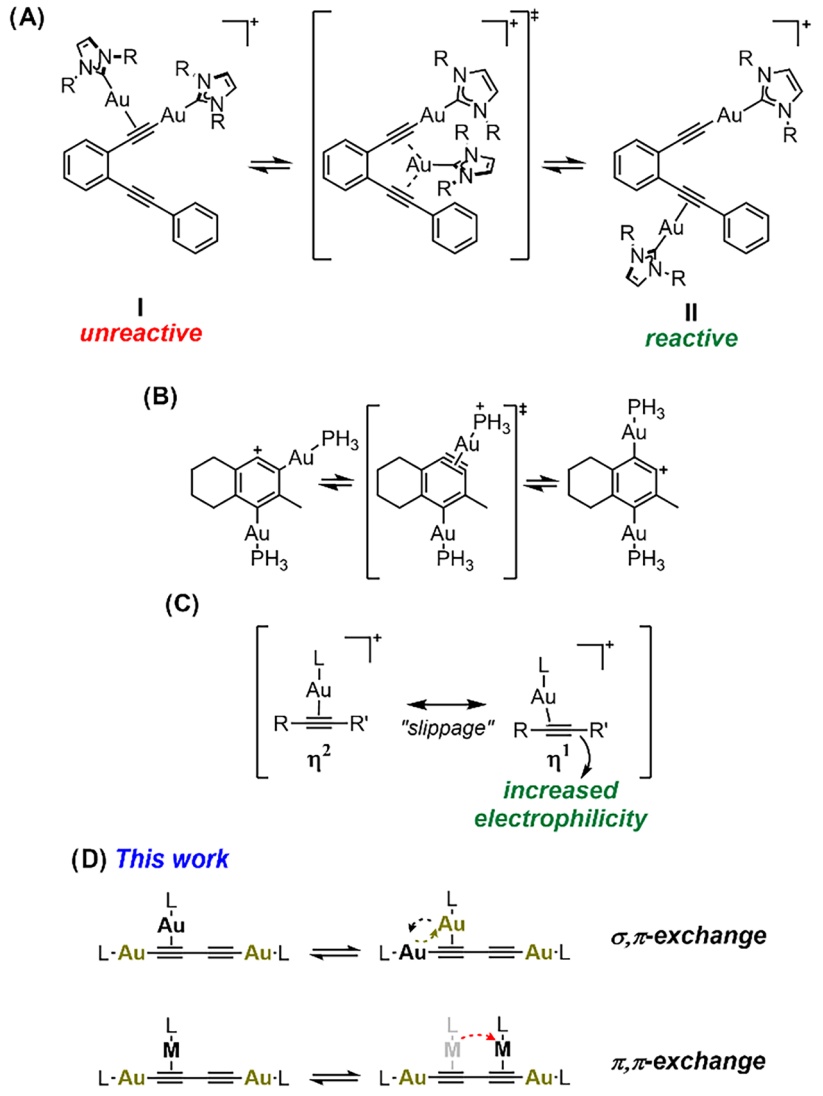

increased electrophilicity of the distal carbon atom (Scheme 1C).[6,9]

While fluxionality has been identified computationally as a widespread, critical process in gold(I) acetylide complexes, to the best of our knowledge, in-depth experimental studies where certain dynamic processes can be thermally arrested are nonexistent, leaving a gap that is essential to investigate for a deeper understanding of the factors that control the electronic properties of these species, and ultimately, their reactivity. For this purpose, we describe in this work the preparation of digold(I) complexes with a variable number of acetylide units and their coordination to IPr−M^+ (M = Au, Cu) fragments to yield the corresponding trimetallic species. These products exhibit σ,π, and/or π,π haptotropic shifts (Scheme 1D), which have been examined in detail both experimentally and computationally.

RESULTS AND DISCUSSION

Previous research from this laboratory concerning migratory insertion reactions on NHC-supported bimetallic gold(I) acetylide complexes involved the synthesis of trinuclear species **1** (Scheme 2 and Figure 1) as part of our mechanistic studies.[10] Cationic trimetallic compound **1** comprises three IPrAu units surrounding an acetylide C_2^{2-} moiety charge-balanced with a triflate anion. In the solid state, two of the IPrAu fragments are σ-bound to the acetylide carbon atoms, while the third metal is π-bound to the C≡C triple bond. However, compound **1** displays dynamic behavior in solution, as only one set of IPr resonances (as opposed to two sets in a 1:2 ratio) is observed by ^{1}H NMR spectroscopy in THF-d_8 at temperatures as low as −95 °C.[10] This observation suggests that a rapid σ,π haptotropic shift occurs, making all of the IPrAu groups chemically equivalent, in line with previously reported σ,π-digold(I) acetylide examples.[4d,5c,11] Thus, in an attempt to arrest this exchange, we carried out VT-NMR experiments over an expanded temperature range. However, slow exchange could not be observed even at −130 °C using $CDCl_2F$ as solvent (Figure S11),[12] indicating that the exchange between the σ and π coordination modes is extremely facile in this complex. Density functional theory (DFT) calculations corroborate this observation, as the calculated Gibbs activation barrier for this process is only 5.3 kcal mol^{-1} (see SI for full computational details).[13] In order to examine how the metal identity may influence the fluxionality

https://doi.org/10.1021/acs.inorgchem.5c04642
Inorg. Chem. 2026, 65, 7153−7160

Scheme 2. Metal Dependence of σ,π-Exchange in Complexes 1 and 3

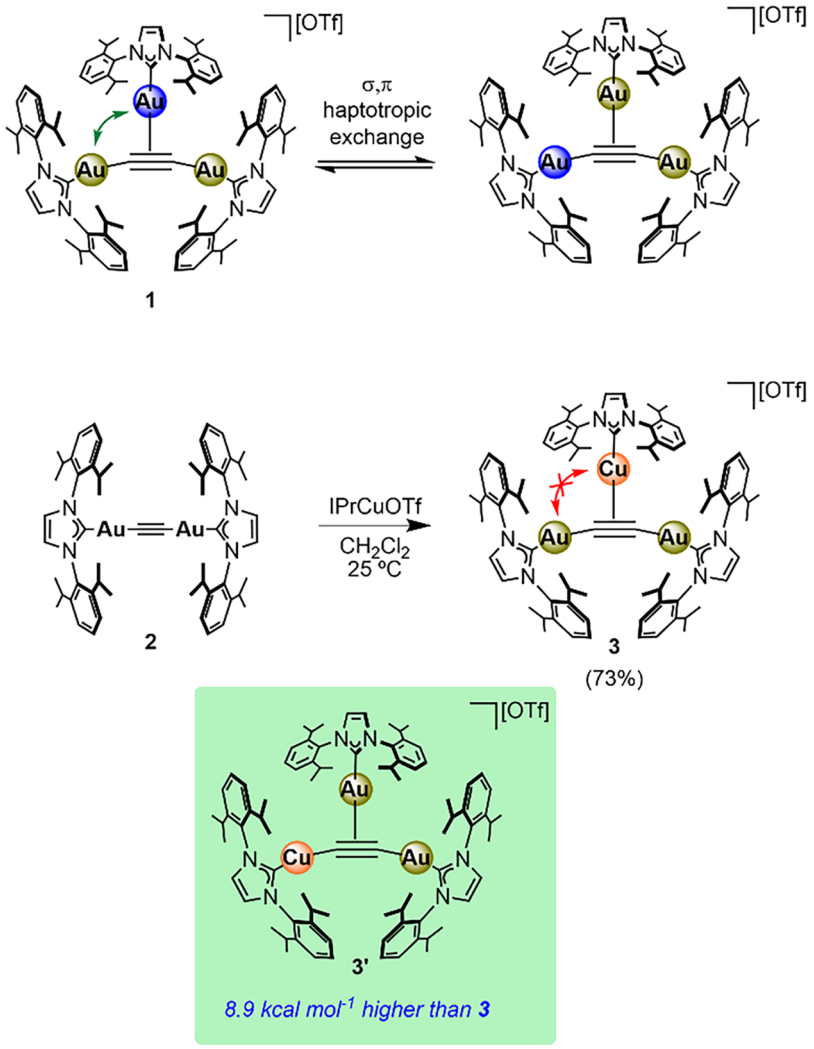

of the resulting complex, a heterometallic analogue was prepared. To this end, 1 equiv of IPrCuOTf was added to a solution of bimetallic acetylide **2** in dichloromethane at 25 °C (Scheme 2); precipitation by addition of *n*-pentane, followed by cooling at −30 °C yielded species **3** in 73% yield.[14]

Structural assignment of trimetallic complex **3** was confirmed by X-ray diffraction studies on single crystals grown by slow diffusion of *n*-pentane into a THF solution of **3** (Figure 1). As with **1**, the $IPrCu^+$ unit of **3** establishes π-bonding with the acetylide moiety in a symmetrical manner (Cu−C1 and Cu−C1′ bond distances ≈ 2.1 Å) with no appreciable metallophilic interactions, given that the Cu···Au distances of 3.5 Å are considerably longer than the sum of their van der Waals radii (3.06 Å).[15] For comparison, similar features are observed for trigold complex **1**, which also presents symmetrical π-bonding (Au−C bond distances ≈ 2.2 Å) and no aurophilic contacts (Au···Au ≈ 3.6−3.7 Å).[10,16] Both solid-state structures exhibit bending of the acetylide Au−C≡C−Au axis (∠Au1−C1−C1′ angles ≈ 161−166°) likely due to the steric congestion attributed to the IPr ligands. Surprisingly, partial scrambling of complex **3** appears to occur from thermal decomposition in solution during the synthesis through an unidentified mechanism. This is evidenced by the cocrystallization of complex **1** within the crystal structure of target compound **3**, based on the 71:29 Cu/Au occupancy at the central metal site in the asymmetric unit (Figure S33). Consistently, ^{1}H NMR spectroscopy presents small amounts (ca. 10%) of complex **1** in the spectrum of species **3**. However, the ^{1}H NMR analysis of **3** at 25 °C reveals two sets of resonances for the IPr ligands in a 2:1 ratio (Figure S1), in agreement with a static structure wherein the $IPrCu^+$ component does not exchange with the σ-bound IPrAu units under these conditions (Scheme 2). Additionally, heating a solution of **3** in 1,2-dichlorobenzene at temperatures up to 125 °C did not appreciably alter the ^{1}H NMR spectrum (Figure S12). These results highlight the stark contrast between the two complexes, as simply changing the central metal atom (despite both being group-11 metals) dramatically affects the fluxional behavior of the system. This seems to be related to the heterometallic nature of the system, given that rapid σ,π exchange has been previously observed for dicopper(I) and tetracopper(I) acetylides.[17] Although the putative isomer **3′** may also be expected to give rise to the observed NMR data (i.e., σ-bound $IPrCu^+$ and two rapidly exchanging IPrAu moieties, Scheme 2), it is 8.9 kcal mol^{-1} higher in energy than complex **3** (according to DFT calculations; the transition state for the σ,π exchange could not be located). These findings are

https://doi.org/10.1021/acs.inorgchem.5c04642
Inorg. Chem. 2026, 65, 7153−7160

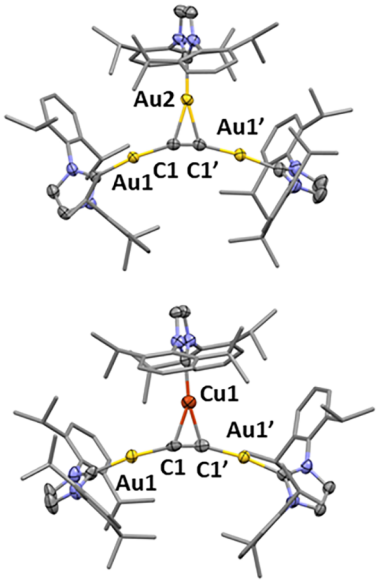

Figure 1. Solid-state structure of trimetallic complexes **1** and **3** (50% probability ellipsoids). H atoms, THF molecules, and OTf anions were omitted, and 2,6-diisopropylphenyl groups were represented as capped sticks for clarity. Partial occupation of Au in the position of Cu1 in complex **3** is not shown.

consistent with the infeasibility of the σ,π exchange process between Cu and Au under the experimental conditions tested.

Motivated by these results, we hypothesized that extending the acetylide linker should increase the number of fluxional processes displayed by these platforms since the presence of two C≡C bonds could potentially lead to π,π haptotropic shifts in addition to the σ,π shifts previously described. Metal π-π exchange has been described in the literature as walking[18] or sliding[19] and is of paramount importance in areas such as molecular switches,[20] the selective activation of C−X bonds,[21] and polymerization processes (catalyst-transfer polycondensation).[22] However, dynamic processes involving π,π exchanges on gold(I) complexes remain unknown.

The extension of the acetylide linker was effected through the synthetic strategy depicted in Scheme 3. Heating of a mixture of trimethylsiloxide complex **4**[23] and 0.5 equiv of 1,4-bis(trimethylsilyl)butadiyne in toluene solution at 120 °C for 4 days led to the selective formation of the target digold(I) diacetylide **5** and hexamethyldisiloxane (HMDSO), as observed by ^{1}H NMR spectroscopy. Species **5** was isolated in 87% yield as an analytically pure beige solid, which readily crystallized from toluene/*n*-pentane mixtures, allowing for its solid-state structure determination via single-crystal X-ray diffraction (Figure 2). The most noticeable feature of its geometry is the slightly bent character of the Au−C≡C−C≡C−Au axis (∠Au1−C1−C2 angle = 170.4(6)°), presumably due to packing effects, given that longer *sp* carbon chains are usually necessary for curved polyyne structures.[24] Similar to acetylide **2**, compound **5** reacts with 1 equiv of either IPrAuOTf or IPrCuOTf to yield the corresponding trinuclear architectures **6** and **7**, respectively, in excellent yields (Scheme 3). The solid-state structures of these complexes were obtained from the X-ray diffraction analysis of single crystals grown by the vapor diffusion of *n*-pentane into THF solutions of each compound (Figure 2). Both structures present the third IPrM$^+$ fragment bound to one of the C≡C bonds of the diacetylide, causing a deviation of the adjacent σ-bound IPrAu moiety away from the linearity with the rest of the C≡C−C≡C−Au axis due to the steric demand of the IPr ligands. While the third gold(I) atom binds an alkyne fragment symmetrically in species **6**, the structure of complex **7** evinces partial slippage of the Cu atom (Figure 2), contrary to some examples in the literature.[6] The addition of 1 equiv of IPrAuOTf to compound **6** in an attempt to install a fourth IPrM$^+$ group did not result in

Scheme 3. Preparation of Complexes 5-7 (Isolated Yields in Parentheses)

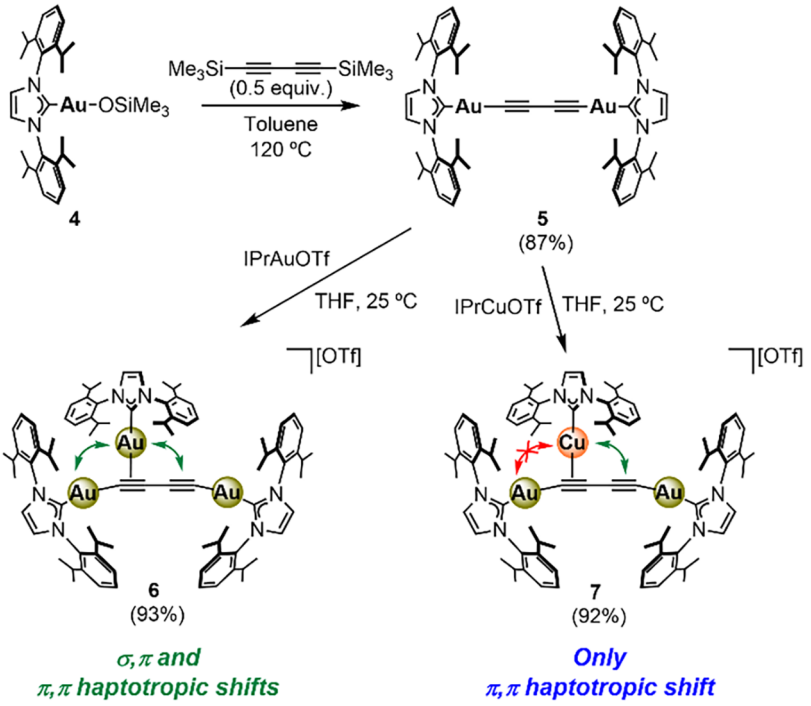

https://doi.org/10.1021/acs.inorgchem.5c04642
Inorg. Chem. 2026, 65, 7153−7160

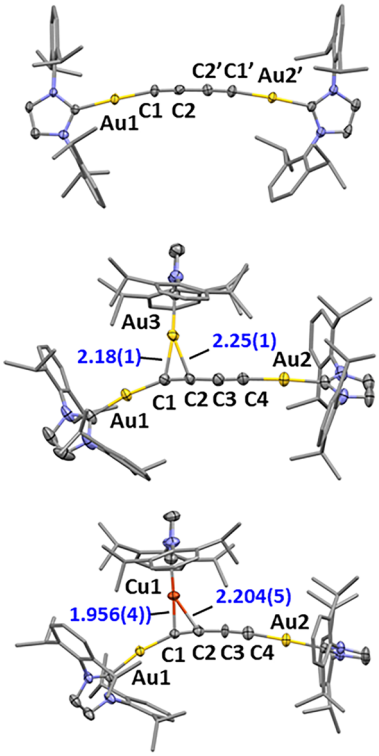

Figure 2. Solid-state structure of complexes **5**, **6**, and **7** (50% probability ellipsoids). H atoms and OTf anions were omitted, and 2,6-diisopropylphenyl groups were represented as capped sticks for the sake of clarity. Only one component of the unit cell of **7** is shown (the other one presents the $IPrCu^+$ fragment approximately perpendicular to that observed in the figure, see Figure S33). Selected bond distances are given in angstroms.

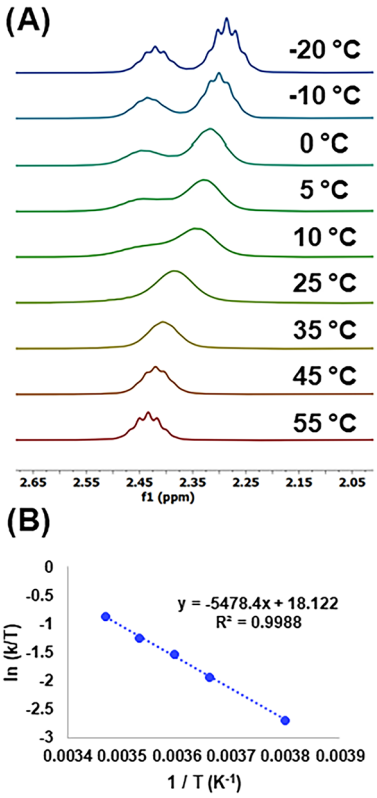

Figure 3. (A) Portion of the variable-temperature ^1H NMR spectra (400 MHz, $CDCl_3$) of complex **6**, corresponding to the methine groups of the IPr ligands. (B) Eyring plot for the π,π-haptotropic shift in complex **6** (ln (k/T) vs 1/T).

any change in the ^1H NMR spectrum. Presumably, the addition of another fragment in this manner is inhibited by the significant steric occlusion about the diyne unit observed in both structures.

In order to investigate the solution state behavior of these π-extended complexes, we employed VT-NMR spectroscopic techniques. The ^1H NMR spectrum of trigold(I) complex **6** in $CDCl_3$ at 25 °C displays coalescence of the IPrAu resonances (Figure S14). Indeed, warming the sample to 55 °C reveals one single set of well-resolved signals for the IPr ligands, consistent with complex **6** exhibiting rapid σ,π and π,π-haptotropic shifts at these temperatures. Conversely, cooling the sample to −10 °C results in the splitting of resonances into two sets of IPr signals with a 2:1 ratio, in agreement with a bonding situation where only the π,π-haptotropic shift has ceased and the σ,π-exchange is still operative (Figure 3). This observation has also been corroborated via NOESY experiments (Figures S22−S24). The ^1H NMR spectrum does not further evolve at lower temperatures (−90 °C in CD_2Cl_2 or −130 °C in $CDCl_2F$), consistent with the dynamic behavior of **1**. In order to rule out alkyne displacement by the triflate anion (as previously reported by Widenhoefer et al.),[11c] **6**·BAr_{24}^F was prepared (BAr_{24}^F = tetrakis[3,5-bis(trifluoromethyl)phenyl]-borate group, see SI). Nonetheless, similar spectra and activation parameters were observed (see Figure S28), ruling out the potential alkyne displacement by the weakly coordinating anion.

Exchange rate constants for the π,π-shift process were extracted from the ^1H NMR spectra (see SI for details),[25] from which an Eyring analysis afforded an activation enthalpy $\Delta H^‡$ = 10.9 ± 0.2 kcal mol^{-1} and an activation entropy $\Delta S^‡$ = −11.2 ± 0.8 cal mol^{-1} K^{-1} (Figure 3). Thus, the Gibbs free energy associated with this process is $\Delta G^‡$ = 14.2 ± 0.2 kcal mol^{-1}. Similar parameters were obtained using methods based on the coalescence temperature (Table S1).[26] DFT calculations are in good agreement with these results, giving $\Delta G^‡$ = 15.7 kcal mol^{-1}, $\Delta H^‡$ = 13.9 kcal mol^{-1}, and $\Delta S^‡$ = −6.2 cal mol^{-1} K^{-1}.

In contrast to that of **6**, the ^1H NMR spectrum of heterometallic complex **7** in CD_2Cl_2 at 25 °C exhibits two sets of resonances for the IPr ligands in a 2:1 ratio. Lowering the temperature in $CDCl_2F$ to −120 °C did not result in any appreciable change in the spectrum that would be consistent with the deceleration of dynamic phenomena. This observation, in combination with the information gathered above for **3** and **6**, points to a facile π,π-haptotropic shift of the $IPrCu^+$ unit along the two triple bonds and the absence of σ,π exchange. Again, transition states and structures derived from potential Au−Cu σ,π exchange in **7** are energetically unfavorable (Figure S41). Warming of compound **7** in 1,2-dichlorobenzene to 105 °C led to the progressive broadening of the $IPrCu^+$ resonances while the diacetylide-bound IPrAu peaks remained unaltered, indicating potential decoordination of $IPrCu^+$ from the π system rather than haptotropic phenomena. As expected, returning to 25 °C gave an identical ^1H NMR spectrum to the starting one (Figure S21). In contrast, the VT-NMR experiment of **3** did not reveal the broadening of any of the resonances during heating, suggesting a tighter binding between $IPrCu^+$ and the triple bond. The computed barrier for the π,π-exchange of the copper(I) fragment in **7** is also

https://doi.org/10.1021/acs.inorgchem.5c04642
Inorg. Chem. 2026, 65, 7153−7160

consistent with the experimental observations, as $\Delta G^{\ddagger}$ = 9.2 kcal mol^{-1}, $\Delta H^{\ddagger}$ = 7.2 kcal mol^{-1}, and $\Delta S^{\ddagger}$ = −6.5 cal mol^{-1} K^{-1}. Therefore, Cu(I) seems to present less difficulty to hop between the two alkyne groups compared to Au(I), and it does not appear to engage in σ,π exchange with gold under the aforementioned experimental conditions.

The more facile metallotropy observed for Cu(I)-containing complex **7** as compared to the analogous Au(I)-only complex **6** can be initially attributed to a weaker interaction between the Cu(I)-NHC moiety and the digold(I) diacetylide **5**, as found in related alkyne complexes.[27] However, energy decomposition analysis-natural orbital for chemical valence (EDA-NOCV) calculations indicate that the intrinsic interaction (ΔE_{int}) between **5** and [IPrCu]$^+$ in complex **7** is nearly identical to that involving [IPrAu]$^+$ in complex **6** (see Table 1). At variance,

Table 1. EDA-NOCV Values (in kcal/mol) for Complexes 6 and 7 and Their Corresponding Transition States TS-6 and TS-7 for the π,π-Haptotropic Shift[a]

	6	TS-6	ΔΔE	7	TS-7	ΔΔE
$\Delta E\ddagger$			12.9			6.5
ΔE_{int}	−107.7	−94.0	13.7	−107.6	−101.2	6.4
ΔE_{Pauli}	139.4	100.4	-39.0	92.9	76.9	-15.9
ΔE_{elstat}	−146.0	−103.9	42.1	−111.7	−91.8	19.9
ΔE_{orb}	−77.4	−65.4	12.0	−65.0	−61.0	4.0
$\Delta E_{orb}(\rho 1)$	−33.4	−24.5	8.9	−24.6	−18.1	6.5
$\Delta E_{orb}(\rho 2)$	−12.3	−6.9	5.4	−9.1	−7.1	2.0
ΔE_{disp}	−23.7	−25.0	**-1.3**	−23.7	−25.2	-1.5

[a]All data have been computed at the ZORA-PBE(0)-D3BJ/DZP//SMD-PBE(0)-D3BJ/6-31G(d,p)&SDD (Cu,Au)

this interaction is much stronger in the transition state associated with the π-π shift involving the Cu(I)-system (**TS-7**). As a result, the change in the interaction energy in going from the initial complex to the corresponding transition state ($\Delta\Delta E_{int}$) is much more pronounced in the Au(I)-only complex than in its Cu(I)-containing counterpart, i.e., $\Delta\Delta E_{int}$ = 13.7 vs 6.4 kcal mol^{-1}, respectively, which matches the total energy difference between the initial species and the corresponding transition structures (ΔE = 12.9 vs 6.5 kcal mol^{-1}), therefore constituting the main factor controlling the different barrier heights in the metallotropic transformation. Partitioning of the crucial ΔE_{int} term into its constituent energy contributors indicates that the lower $\Delta\Delta E_{int}$ computed for the Cu(I)-containing system does not originate from the change in the Pauli repulsion ($\Delta\Delta E_{Pauli}$ = −15.9 vs −39.0 kcal mol^{-1} for the Cu(I)-containing and Au(I)-only species, respectively) but from smaller differences in electrostatic interactions ($\Delta\Delta E_{elstat}$ = 19.9 vs 42.1 kcal mol^{-1}) and, to a lesser extent, also from smaller differences in orbital interactions ($\Delta\Delta E_{orb}$ = 4.0 vs 12.0 kcal mol^{-1}, respectively), including both the σ-donation ($\rho 1$) and the π-backdonation ($\rho 2$). The smaller differences in electrostatic interactions have also been supported via molecular electrostatic potential (MESP) distribution and charge analysis (see Figure S42).[28] These results therefore suggest that the lower barrier observed for the π-π metallotropy involving **7** is not dominated by the interaction between the individual fragments in the initial complexes but by the change of these interactions as the transition states are reached.

CONCLUDING REMARKS

In conclusion, this work describes the preparation of group-11-based trimetallic mono- and diacetylide complexes and the investigation of their dynamic behavior in solution. While σ,π-exchange phenomena in gold-only complexes **1** and **6** seem to be extremely facile even at −130 °C, the copper-containing complexes of **3** and **7** do not appear to exhibit σ,π shifts under the experimental conditions tested. On the other hand, π,π metallotropic shifts are observed in the synthesized diacetylide species for both gold and copper-containing units. Whereas the π,π-shift of copper in compound **7** cannot be thermally arrested at low temperatures, this process can be halted in trigold complex **6** at −10 °C. The stark difference between both complexes is computationally supported to reside in the higher electrostatic and orbital energy changes necessary for complex **6** to achieve the transition state geometry. These results demonstrate how the nature of the metal has a pronounced repercussion in the resulting fluxional character of a certain chemical system, which can be of interest from the point of view of molecular machines. Additionally, these findings provide the first experimental evidence for a dynamic process in which the gold moiety can be thermally "localized" on one region of the alkynyl-containing molecule, as it is no longer able to alternate between the triple bonds. These findings might have implications from the perspective of homogeneous catalysis, as thermal control and/or metal identity can drive the selectivity of a certain transformation.[29] On the other hand, the mobility of NHC−M$^+$ fragments along a carbon chain can be regarded as a molecular model of NHC-gold adatoms or adsorbed metals on surfaces,[30] whose motion is critical in the formation of self-assembled monolayers (SAMs).

EXPERIMENTAL DETAILS

Unless stated otherwise, all reactions were performed in a glovebox or on a Schlenk line under an atmosphere of pure Ar or high-purity N_2 by using standard Schlenk techniques. All solvents were dried and degassed prior to use. C_6D_6 was distilled under Ar and stored over 3 Å molecular sieves for at least 24 h prior to use. $CDCl_3$, CD_2Cl_2, and 1,2-dichlorobenzene were dried over calcium hydride before being distilled and degassed by three freeze−pump−thaw cycles. IPrAuOTf,[29] IPrCuOTf,[31] $CDCl_2F$,[12] and complexes **1**[10] and **4**[23] were prepared according to literature procedures. All other reagents were purchased from commercial suppliers and used as received. $CDCl_2F$ was distilled and stored over 3 Å molecular sieves in a sealed vessel at −24 °C. No uncommon hazards are noted for the experimental work described in this article.[32]

ASSOCIATED CONTENT

Supporting Information

The Supporting Information is available free of charge at https://pubs.acs.org/doi/10.1021/acs.inorgchem.5c04642.

Computed species (XYZ)

Material including synthetic, spectroscopic, crystallographic, and computational details (PDF)

Accession Codes

Deposition Numbers 2475549−2475552 contain the supplementary crystallographic data for this paper. These data can be obtained free of charge via the joint Cambridge Crystallographic Data Centre (CCDC) and Fachinformationszentrum Karlsruhe Access Structures service.

https://doi.org/10.1021/acs.inorgchem.5c04642
Inorg. Chem. 2026, 65, 7153−7160

AUTHOR INFORMATION

Corresponding Authors

Israel Fernández − *Departamento de Química Orgánica I and Centro de Innovación en Química Avanzada (ORFEO−CINQA), Facultad de Químicas, Universidad Complutense de Madrid, Madrid 28040, Spain;* orcid.org/0000-0002-0186-9774; Email: israel@quim.ucm.es

Pablo Ríos − *Instituto de Investigaciones Químicas (IIQ), Departamento de Química Inorgánica, Centro de Innovación en Química Avanzada (ORFEO−CINQA), CSIC and Universidad de Sevilla, 41092 Sevilla, Spain;* orcid.org/0000-0003-4467-4157; Email: prios1@us.es

Authors

Ignacio Nieto-Vargas − *Instituto de Investigaciones Químicas (IIQ), Departamento de Química Inorgánica, Centro de Innovación en Química Avanzada (ORFEO−CINQA), CSIC and Universidad de Sevilla, 41092 Sevilla, Spain*

Juan Cayuela-Castillo − *Instituto de Investigaciones Químicas (IIQ), Departamento de Química Inorgánica, Centro de Innovación en Química Avanzada (ORFEO−CINQA), CSIC and Universidad de Sevilla, 41092 Sevilla, Spain*

Francisco J. Fernández-de-Córdova − *Instituto de Investigaciones Químicas (IIQ), Departamento de Química Inorgánica, Centro de Innovación en Química Avanzada (ORFEO−CINQA), CSIC and Universidad de Sevilla, 41092 Sevilla, Spain;* orcid.org/0000-0002-1784-2840

Complete contact information is available at: https://pubs.acs.org/10.1021/acs.inorgchem.5c04642

Notes

The authors declare no competing financial interest.

ACKNOWLEDGMENTS

This work was supported by the Junta de Andalucía under project ProyExcel_00758. We are also grateful for financial support from grants PID2024-160351NA-I00, PID2022-139318NB-I00, RED2022-134331-T, and RED2022-134287-T funded by MICIU/AEI/10.13039/501100011033. We thank Dr. Matthew S. See, Dr. Amor Rodríguez, Dr. Salvador Conejero, Dr. T. Alexander Wheeler, and Prof. Rex C. Handford for useful discussions during the preparation of this manuscript. We also thank Dr. Jesús Angulo for his assistance with NOESY experiments.

REFERENCES

(1) Hashmi, A. S. K. Gold-Catalyzed Organic Reactions. *Chem. Rev.* **2007**, *107*, 3180−3211.

(2) Cheong, P. H-Y.; Morganelli, P.; Luzung, M. R.; Houk, K. N.; Toste, F. D. Gold-Catalyzed Cycloisomerization of 1,5-Allenynes via Dual Activation of an Ene Reaction. *J. Am. Chem. Soc.* **2008**, *130*, 4517−4526.

(3) (a) Hashmi, A. S. K. Dual Gold Catalysis. *Acc. Chem. Res.* **2014**, *47*, 864−876. (b) Zhao, X.; Rudolph, M.; Hashmi, A. S. K. Dual gold catalysis - an update. *Chem. Commun.* **2019**, *55*, 12127−12135.

(4) Selected examples: (a) Odabachian, Y.; Le Goff, X. F.; Gagosz, F. An Unusual Access to Medium Sized Cycloalkynes by a New Gold(I)-Catalysed Cycloisomerisation of Diynes. *Chem. - Eur. J.* **2009**, *15*, 8966−8970. (b) Ye, L.; Wang, Y.; Aue, D. H.; Zhang, L. Experimental and Computational Evidence for Gold Vinylidenes: Generation from Terminal Alkynes via a Bifurcation Pathway and Facile C−H insertions. *J. Am. Chem. Soc.* **2012**, *134*, 31−34. (c) Wang, Y.; Yepremyan, A.; Ghorai, S.; Todd, R.; Aue, D. H.; Zhang, L. Gold-Catalyzed Cyclizations of *cis*-Enediynes: Insights into the Nature of Gold-Aryne Interactions. *Angew. Chem., Int. Ed.* **2013**, *52*, No. 7795. (d) Hashmi, A. S. K.; Lauterbach, T.; Nösel, P.; Vilhelmsen, M. H.; Rudolph, M.; Rominger, F. Dual Gold Catalysis: σ,π-Propyne Acetylide and Hydroxyl-Bridged Digold Complexes as Easy-To-Prepare and Easy-To-Handle Precatalysts. *Chem. - Eur. J.* **2013**, *19*, 1058−1065. (e) Hansmann, M. M.; Rudolph, M.; Rominger, F.; Hashmi, A. S. K. Mechanistic Switch in Dual Gold Catalysis of Diynes: C(sp^3)−H Activation through Bifurcation − Vinylidene versus Carbene Pathways. *Angew. Chem., Int. Ed.* **2013**, *52*, 2593−2598. (f) Vachhani, D. D.; Galli, M.; Jacobs, J.; Meervelt, L. V.; Van der Eycken, E. V. Synthesis of (spiro)cyclopentapyridinones *via* C_{sp3}−H functionalization: a post-Ugi gold-catalyzed regioselective tandem cyclization. *Chem. Commun.* **2013**, *49*, 7171−7173. (g) Ranieri, B.; Escofet, I.; Echavarren, A. M. Anatomy of gold catalysts: facts and myths. *Org. Biomol. Chem.* **2015**, *13*, 7103−7118.

(5) Selected examples: (a) Simonneau, A.; Jaroschik, F.; Lesage, D.; Karanik, M.; Guillot, R.; Malacria, M.; Tabet, J.-C.; Goddard, J.-P.; Fensterbank, L.; Gandon, V.; Gimbert, Y. Tracking gold acetylides in gold(I)-catalyzed cycloisomerization reactions of enynes. *Chem. Sci.* **2011**, *2*, 119−147. (b) Brown, T. J.; Weber, D.; Gagné, M. R.; Widenhoefer, R. A. Mechanistic Analysis of Gold(I)-Catalyzed Intramolecular Allene Hydroalkoxylation Reveals an Off-Cycle Bis(gold) Vinyl Species and Reversible C−O Bond Formation. *J. Am. Chem. Soc.* **2012**, *134*, 9134−9137. (c) Ferrer, S.; Echavarren, A. M. Role of σ,π-Digold(I) Alkyne Complexes in Reactions of Enynes. *Organometallics* **2018**, *37*, 781−786.

(6) Shapiro, N. D.; Toste, F. D. Synthesis and structural characterization of isolable coinage metal π-complexes. *Proc. Natl. Acad. Sci. U.S.A.* **2008**, *105*, 2779−2782.

(7) Gimeno, A.; Cuenca, A. B.; Suárez-Pantiga, S.; Ramírez de Arellano, C.; Medio-Simón, M.; Asensio, G. Competitive Gold-Activation Modes in Terminal Alkynes: An Experimental and Mechanistic Study. *Chem. - Eur. J.* **2014**, *20*, 683−688.

(8) Vilhelmsen, M. H.; Hashmi, A. S. K. Reaction Mechanism for the Dual Gold-Catalyzed Synthesis of Dibenzopentalene: A DFT Study. *Chem. - Eur. J.* **2014**, *20*, 1901−1908.

(9) (a) Fürstner, A.; Davies, P. W. Catalytic Carbophilic Activation: Catalysis by Platinum and Gold π Acids. *Angew. Chem., Int. Ed.* **2007**, *46*, 3410−3449. (b) Rocchigiani, L.; Fernandez-Cestau, J.; Agonigi, G.; Chambrier, I.; Budzelaar, P. H. M.; Bochmann, M. Gold(III) Alkyne Complexes: Bonding and Reaction Pathways. *Angew. Chem., Int. Ed.* **2017**, *56*, 13861−13865. (c) Bruggeman, H. E.; Lorson, R.; Allen, L. J.; Jackson, L. G.; Gee, W.; Haines, B. E. A Computational Study of Gold(I)-Catalyzed Isomerization of Cyclooctyne: A Case Study on the Mechanism of C(sp^3)−H Insertion by Cationic Gold Alkyne Complexes and Model Studies. *Organometallics* **2024**, *43*, 2147−2157.

(10) Cayuela-Castillo, J.; Fernández-de-Córdova, F. J.; See, M. S.; Fernández, I.; Ríos, P. Stepwise alkyne insertion in Au(I) acetylides: influence of the nuclearity. *Chem. Sci.* **2025**, *16*, 4684−4694.

(11) Selected examples: (a) Hooper, T. N.; Green, M.; Russell, C. A. Cationic Au(I) alkyne complexes: synthesis, structure and reactivity. *Chem. Commun.* **2010**, *46*, 2313−2315. (b) Himmelspach, A.; Finze, M.; Raub, S. Tetrahedral Gold(I) Clusters with Carba-*closo*-dodecaboranylethynido Ligands: [{12-$(R_3PAu)_2$C≡C-*closo*-1-$CB_{11}H_{11}$}$_2$]. *Angew. Chem., Int. Ed.* **2011**, *50*, 2628−2631. (c) Brown, T. J.; Widenhoefer, R. A. Cationic Gold(I) π-Complexes of Terminal Alkynes and Their Conversion to Dinuclear σ,π-Acetylide Complexes. *Organometallics* **2011**, *30*, 6003−6009.

(12) Siegel, J. S.; Anet, F. A. L. Dichlorofluoromethane-*d*: A Versatile Solvent for VT-NMR Experiments. *J. Org. Chem.* **1988**, *53*, 2629−2630.

(13) DFT calculations performed in reference10 were carried out using a smaller basis set, which explains the difference in energy values.

(14) The solid obtained presents small amounts of complex **1**, as observed both in the crystal structure and by NMR analysis. See main text and Supporting Information for more details.

(15) Bondi, A. van der Waals Volumes and Radii. *J. Phys. Chem. A* **1964**, *68*, 441−451.
(16) Schmidbaur, H. The Aurophilicity Phenomenon: A Decade of Experimental Findings, Theoretical Concepts and Emerging Applications. *Gold Bull.* **2000**, *33*, 3−10.
(17) (a) Lo, W.-Y.; Lam, C.-H.; Fung, W. K-M.; Sun, H.-Z.; Yam, V. W-W.; Balcells, D.; Maseras, F.; Eisenstein, O. An oscillating C_2^{2-} unit inside a copper rectangle *Chem. Commun.* 2003, p 1260. (b) Jin, L.; Tolentino, D. R.; Melaimi, M.; Bertrand, G. Isolation of bis(copper) key intermediates in Cu-catalyzed azide-alkyne "click reaction". *Sci. Adv.* **2015**, *1*, No. e1500304.
(18) In order to avoid confusion, we will not describe π,π-haptotropic shifts as walking, since it can be misunderstood with chain-walking processes mediated by gold, such as those described for example in Bhoyare, V. W.; Tathe, A. G.; Gandon, V.; Patil, N. T. Unlocking the Chain-Walking Process in Gold Catalysis. *Angew. Chem., Int. Ed.* **2023**, *62*, No. e202312786.
(19) Huidobro-Meezs, I. L.; Segovia-Poncelis, M.; Barquera-Lozada, J. E. The Role of Bulkiness in Haptotropic Shifts of Metal-Cumulene Complexes. *Eur. J. Inorg. Chem.* **2016**, *2016*, 4226−4233.
(20) Jahr, H. C.; Nieger, M.; Dötz, K. H. Controlled haptotropic rearrangements − towards a stereospecific molecular switch based on chiral arene chromium complexes. *Chem. Commun.* **2003**, 2866−2867.
(21) Selected references: (a) Strawser, D.; Karton, A.; Zenkina, O. V.; Iron, M. A.; Shimon, L. J. W.; Martin, J. M. L.; van der Boom, M. E. Platinum Stilbazoles: Ring-Walking Coupled with Aryl−Halide Bond Activation. *J. Am. Chem. Soc.* **2005**, *127*, 9322−9323. (b) Zenkina, O. V.; Karton, A.; Freeman, D.; Shimon, L. J. W.; Martin, J. M. L.; van der Boom, M. E. Directing Aryl−I versus Aryl−Br Bond Activation by Nickel via a Ring Walking Process. *Inorg. Chem.* **2008**, *47*, 5114−5121. (c) Zenkina, O. V.; Gidron, O.; Shimon, L. J. W.; Iron, M. A.; van der Boom, M. E. Mechanistic Aspects of Aryl-Halide Oxidative Addition, Coordination Chemistry, and Ring-Walking by Palladium. *Chem. - Eur. J.* **2015**, *21*, 16113−16125.
(22) Selected references: (a) Miyakoshi, R.; Yokoyama, A.; Yokozawa, T. Catalyst-Transfer Polycondensation. Mechanism of Ni-Catalyzed Chain-Growth Polymerization Leading to Well-Defined Poly(3-hexylthiophene). *J. Am. Chem. Soc.* **2005**, *127*, 17542−17547. (b) Tkachov, R.; Senkovskyy, V.; Komber, H.; Sommer, J.-U.; Kiriy, A. Random Catalyst Walking around Polymerized Poly(3-hexylthiophene) Chains in Kumada Catalyst-Transfer Polycondensation. *J. Am. Chem. Soc.* **2010**, *132*, 7803−7810. (c) Mikami, K.; Nojima, M.; Masumoto, Y.; Mizukoshi, Y.; Takita, R.; Yokozawa, T.; Uchiyama, M. Catalyst-dependent intrinsic ring-walking behavior on π-face of conjugated polymers. *Polym. Chem.* **2017**, *8*, 1708−1713.
(23) Robilotto, T. J.; Bacsa, J.; Gray, T. G.; Sadighi, J. P. Synthesis of a Trigold Monocation: An Isolobal Analogue of $[H_3]^+$. *Angew. Chem., Int. Ed.* **2012**, *51*, 12077−12080.
(24) Dembinski, R.; Lis, T.; Szafert, S.; Mayne, C. L.; Bartik, T.; Gladysz, J. A. Appreciably bent *sp* carbon chains: synthesis, structure, and protonation of organometallic 1,3,5-triynes and 1,3,5,7-tetraynes of the formula $(\eta^5\text{-}C_5Me_5)Re(NO)(PPh_3)((C{\equiv}C)_n\text{-}p\text{-}C_6H_4Me)$. *J. Organomet. Chem.* **1999**, *578*, 229−246.
(25) (a) Sandström, J. *Dynamic NMR Spectroscopy*; Academic Press: London, 1982; pp 77−92. (b) Gasparro, F. P.; Kolodny, N. H. NMR Determination of the Rotational Barrier in N,N-dimethylacetamide. *J. Chem. Educ.* **1977**, *54*, No. 258.
(26) Huggins, M. T.; Kesharwani, T.; Buttrick, J.; Nicholson, C. Variable Temperature NMR Experiment Studying Restricted Bond Rotation. *J. Chem. Educ.* **2020**, *97*, 1425−1429.
(27) Das, A.; Dash, C.; Celik, M. A.; Yousufuddin, M.; Frenking, G.; Rasika Dias, H. V. Tris(alkyne) and Bis(alkyne) Complexes of Coinage Metals: Synthesis and Characterization of $(cyclooctyne)_3M^+$ (M = Cu, Ag) and $(cyclooctyne)_2Au^+$ and Coinage Metal (M = Cu, Ag, Au) Family Group Trends. *Organometallics* **2013**, *32*, 3135−3144.
(28) Thushara, R.; Koga, N.; Suresh, C. H. Gold(I) Catalysis in Alkyne-Alkene Reactions: A Systematic Exploration through Molecular Electrostatic Potential Analysis. *Inorg. Chem.* **2024**, *63*, 17406−17417.
(29) For a particular case where both Cu and Au are involved in a catalytic transformation, see Lazreg, F.; Guidone, S.; Gómez-Herrera, A.; Nahra, F.; Cazin, C. S. J. Hydrophenoxylation of internal alkynes catalysed with a heterobimetallic Cu-NHC/Au-NHC system. *Dalton Trans.* **2017**, *46*, 2439−2444.
(30) Wang, G.; Rühling, A.; Amirjalayer, S.; Knor, M.; Ernst, J. B.; Richter, C.; Gao, H.-J.; Timmer, A.; Gao, H.-Y.; Doltsinis, N. L.; Glorius, F.; Fuchs, H. Ballbot-type motion of N-heterocyclic carbenes on gold surfaces. *Nat. Chem.* **2017**, *9*, 152−156.
(31) Cheng, L.-J.; Cordier, C. J. Catalytic Nucleophilic Fluorination of Secondary and Tertiary Propargylic Electrophiles with a Copper-N-Heterocyclic Carbene Complex. *Angew. Chem., Int. Ed.* **2015**, *54*, 13734−13738.
(32) Part of this work was previously submitted to ChemRxiv: Nieto-Vargas, I.; Cayuela-Castillo, J.; Fernández-de-Córdova, F. J.; Fernández, I.; Ríos, P. Haptotropic phenomena in digold(I) triple-bonded complexes. *ChemRxiv*, 2025 DOI: 10.26434/chemrxiv-2025-63h9j.

https://doi.org/10.1021/acs.inorgchem.5c04642
Inorg. Chem. 2026, 65, 7153−7160